

pubs.acs.org/Macromolecules Article

Efficient Near-Infrared Photopolymerizations Using azaBODIPYs with Electron-Donating Groups and Intramolecular Charge Transfer

Alex Stafford, Seth R. Allen, Laura Estergreen, Kristina Kafle, Sean T. Roberts,* and Zachariah A. Page*



Cite This: *Macromolecules* 2023, 56, 9804–9810



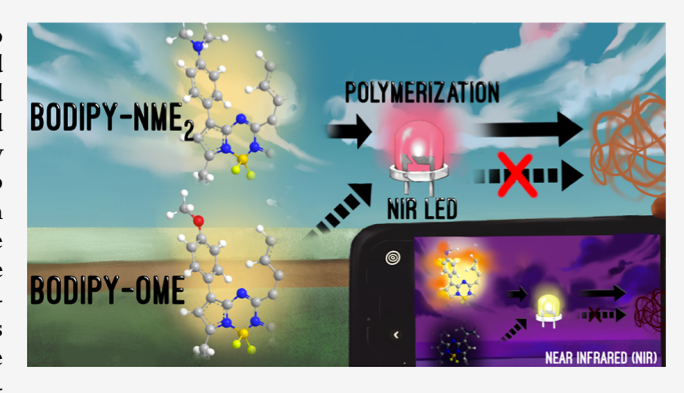
ACCESS

III Metrics & More

Article Recommendations

Supporting Information

ABSTRACT: Polymerizations driven by low-energy, far-red to near-infrared (NIR) light can enable mild, biocompatible, and wavelength-selective photocuring for the fabrication of advanced soft materials. This arises from a reduction in light scattering and photodamage by long-wavelength light relative to commonly employed UV light. However, photopolymerizations with far-red to NIR light are slow and inefficient and thus require long reaction times, high light intensities, and/or large catalyst loadings relative to analogous UV light-driven approaches. To overcome these limitations, a comprehensive evaluation of aza-boron dipyrromethene (azaBODIPY) derivatives as far-red to NIR reactive catalysts to efficiently induce polymerizations is presented. Herein, we examine how introducing electron-donating groups into azaBO-



DIPY scaffolds affects the polymerization rate (r_p) . The systematic introduction of methoxy functionality resulted in a ~5× increase in r_p upon exposure to a far-red (740 nm) LED, along with unprecedented sensitivity (0.7 mW/cm², $r_p = 0.1$ M/s), while maintaining good temporal control over photopolymerization. Replacing methoxy groups with more electron-donating dimethylamino groups enhanced the charge transfer (CT) character of photoexcited azaBODIPY molecules, which enabled NIR light-driven polymerizations with low intensity LED exposure (850 nm, ~55 mW/cm², $r_p = 0.1$ M/s). Furthermore, transient absorption spectroscopy revealed a direct relationship between the lifetime of azaBODIPY CT states and r_p , which revealed that azaBODIPYs bearing dimethylamino functionality at the aza-bridgehead side of the molecule are optimal for photopolymerization. The unveiled catalyst design principles will inform next-generation NIR light-fueled photopolymerizations and enable integration with emergent additive manufacturing technologies.

■ INTRODUCTION

The utility of light as an energy source to rapidly convert liquid resins into solid structures has found broad applications in imaging and curing technologies, such as lithography, adhesives, coatings, and 3D printing. However, contemporary light-based manufacturing relies on high-energy UV light, which limits the scope of materials that can be produced due to pervasive absorption and scattering. For example, UV (<400 nm) light is often incompatible with biomedical applications due to its shallow penetration depth through tissue and the risk of cellular damage upon absorption.9 The benefits of photocuring with visible and near-infrared (NIR) light include (1) mild and more cost-effective conditions, (2) deeper light penetration, and (3) spectral control (i.e., the ability to activate discrete chemical pathways using specific wavelengths of light). 10-12 However, as the wavelength of light increases, the energy packed within each photon decreases, concomitantly reducing their potential to initiate polymerization. This results in longer times to solidification, precluding the use of visible-to-NIR light in the aforementioned applications that often require curing in under ~60 s or a polymerization rate on the order of ~ 0.1 M/s at modest light intensities ($\lesssim 50$ mW/

cm²) to be practical. Although recent progress has been made in improving the efficiency (e.g., speed and sensitivity) of visible-to-NIR photocuring, ^{13–20} including for use in 3D printing, ^{21–23} novel photocatalyst systems and greater fundamental insights into their design principles are required to consider implementation in commercially relevant photocuring technologies.

Photocuring systems that operate using light with wavelengths of ≥500 nm (green light or redder) typically operate by photoinduced electron/energy transfer (PET) mechanisms (type II reactions). This is in contrast with direct photolysis reactions (type I reactions) that can be driven by using shorter wavelengths of light (primarily UV). To facilitate PET, two- or three-component photosystems are common. These multi-

Received: October 2, 2023 Revised: November 11, 2023 Accepted: November 15, 2023 Published: December 1, 2023





component photosystems are composed of a photocatalyst (PC) and an electron-rich donor (D) and/or electron deficient acceptor (A) that act as (co) initiators to generate reactive radical species upon irradiation with light.

Traditionally, xanthenes and cyanines have dominated the literature for use as green/red- and red/NIR-light activated PCs, respectively. 18,24,25 For example, Lalevée and co-workers^{26,27} recently showed that a cyanine-borate salt could be used for rapid polymerization upon exposure to a NIR laser diode (785 nm) at an intensity of 2.55 W/cm², resulting in ~40 s exposure times to reach maximum monomer conversion. Using the same NIR laser diode at an intensity of 400 mW/ cm², they demonstrated polymerizations with squaraine, squarylium, and BODIPY dyes, reaching maximum monomer conversion after \sim 140, \sim 120, and \sim 200 s, respectively. In concert with our efforts reported here, Allonas and coworkers, ²⁸ synthesized a penta-methine cyanine dye that could achieve NIR photopolymerization within ~10 s at 40 mW/cm² using a NIR LED centered at 850 nm. However, this system relied on the formation of a complex between the cationic dye and an anionic electron donor, which can introduce challenges, as solubility constraints of charged dyes often necessitate dilution of photopolymer resins with solvent. Thus, further systematic development and characterization of novel longwavelength reactive photoredox catalyst systems are needed to develop resins that are compatible with modern stereolithography platforms where exposure power may be limited (e.g., projection/display-based 3D printing).

To improve visible light photocuring efficiency, we recently examined a unique three-component photosystem comprising halogenated boron dipyromethene (BODIPY) and azaBODI-PY dyes as PCs, where a triphenyl(n-butyl) borate and diphenyliodonium salt served as electron donors and acceptors, respectively. Upon exposure to LEDs centered at 525 nm (green) and 740 nm (far-red), a maximum monomer conversion was achieved within ~ 60 s (~ 0.1 M/s) using light intensities as low as ~ 0.05 and ~ 5.0 mW/cm², respectively. Critically, the halogens (Br and I) facilitated intersystem crossing (ISC) to a long-lived triplet excited state, which inturn improved the photocuring efficiency. While this enabled rapid visible light photocuring, a photosystem operable at NIR wavelengths (≥ 780 nm) via exposure from energy-efficient LEDs remained elusive.

Herein, we systematically examine the effects of electrondonating groups (EDGs) and halogenation on the photocuring efficiency of far-red to NIR-absorbing azaBODIPY PCs (Figure 1). The particular derivates we examine were inspired by recent work of Zhao and co-workers³⁰ as well as Łapok and coworkers³¹ wherein aza-BODPYs bearing strong electrondonating para-(dimethylamino)phenyl substituents showed efficient NIR absorption, unique intramolecular charge transfer (CT) characteristics, and ISC to long-lived triplet excited states upon halogenation. Using these materials as PCs, we demonstrate high photopolymerization efficiencies using farred (0.1 M/s at 0.7 mW/cm², 740 nm) and NIR (0.1 M/s at 55 mW/cm², 850 nm) LEDs, while maintaining excellent temporal control (i.e., no initial dark polymerization). Additionally, ultrafast transient absorption (TA) spectroscopy revealed that NIR photopolymerizations are uniquely enabled by intramolecular CT states and that the lifetimes of these states directly correlate with the photopolymerization efficiency. We anticipate that the design principles we report

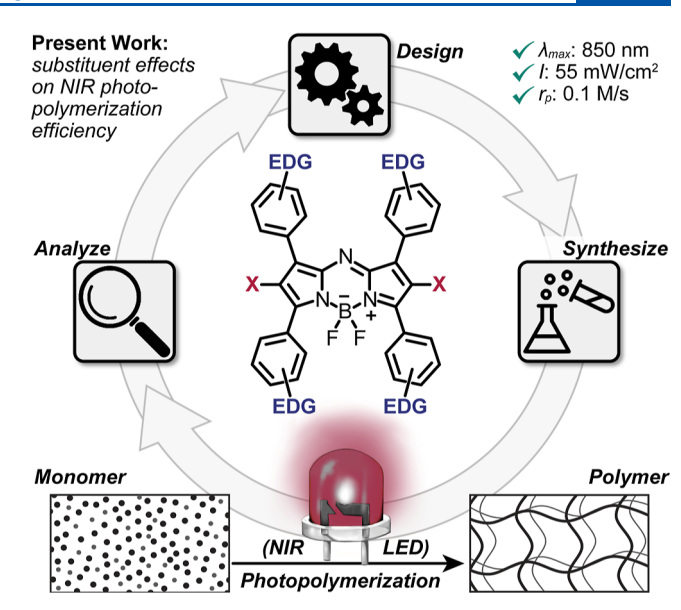


Figure 1. Enhancing photopolymerization efficiency fueld by NIR light. Systematic design-synthesis-analysis circularity with azaBODIPY derivatives as photocatalysts enabled high polymerization rates $(r_{\rm p})$ using low-intensity (I) light-emitting diodes having an emission wavelength maximum $(\lambda_{\rm max})$ of 850 nm.

can be used to further improve long-wavelength visible-to-NIR photocuring toward its implementation in industrial processes.

■ RESULTS AND DISCUSSION

Synthesis and Absorption. A library of azaBODIPY derivatives bearing EDGs were prepared and tested as PCs owing to their ease of synthesis, high extinction coefficients $(>5 \times 10^4 \text{ M}^{-1} \text{ cm}^{-1})$ in the far-red to NIR spectral region (≥700 nm), and potential biocompatibility.³²⁻³⁶ Specifically, the azaBODIPYs contained phenyl rings with tertiary-butyl, methoxy, and/or dimethylamino functionality (Figure 2A). Although the library contains 11 BODIPY derivatives, for clarity, only a subset is described in the main text (7 total) to draw key structure-reactivity relationships. Supplemental compounds that reinforce these claims are provided in the Supporting Information (Scheme S1). The naming convention used herein is as follows: ("top" EDGs)-("bottom" EDGs)azaX, where top refers to the pyrrole site nearest to the nitrogen bridgehead (R1, Figure 2A), bottom refers to the pyrrole site nearest to the boron (R², Figure 2A), and X refers to pyrrole functionalization at the 3-position with hydrogen (H) or bromine (Br). For example, (MeO)₃-tBu-azaBr represents a control compound that we previously reported as a highly efficient PC for light-induced free radical polymerizations using far-red LEDs, centered at 740 nm.²⁵

The large library of compounds was made possible by the modularity of the synthetic scheme we employ, which followed a straightforward four- or five-step protocol (Scheme S1). Briefly, aldol condensation of the respective EDG benzaldehyde and acetophenone was performed under basic conditions, followed by a Michael addition with nitromethane. The azadipyrromethene was obtained in one pot by using ammonium acetate in ethanol under reflux. The reaction with BF₃·OEt₂ yielded the desired azaBODIPY derivatives. Subsequent reactions with NBS resulted in the brominated azaBODIPY (see the Supporting Information for more details). The

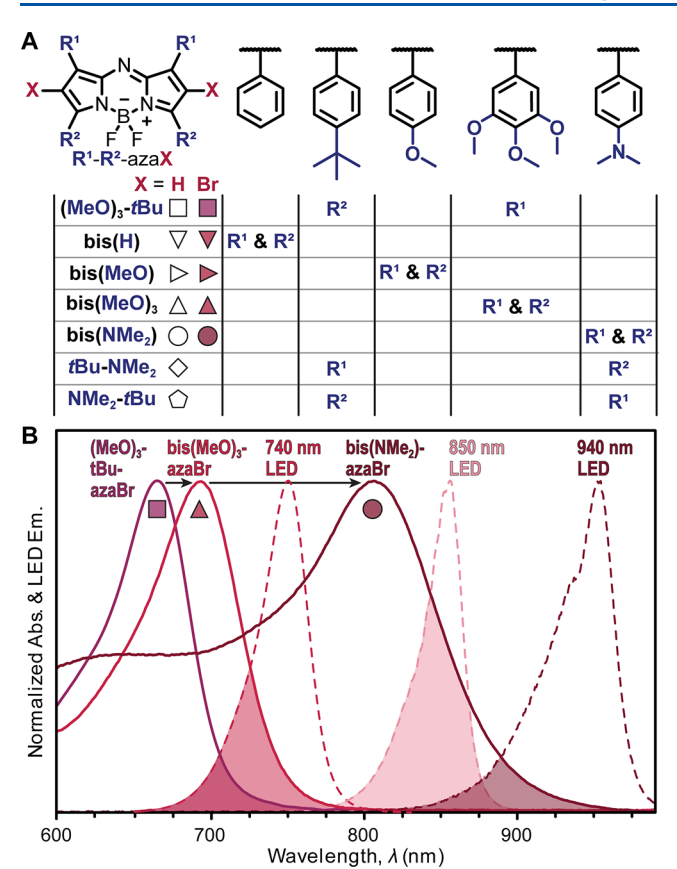


Figure 2. Representative chemical structures (A) and absorption profiles (B) for halogenated azaBODIPYs. Absorbance was normalized and overlaid with 740, 850, and 940 nm LED emission profiles used in this study; cross sections are shaded.

tunability of this protocol provides a means to further modify and study BODIPY derivatives as PCs.

The absorption profiles and associated extinction coefficients of synthesized azaBODIPYs were characterized using UV-vis absorption spectroscopy to determine their spectral overlap with far-red and NIR light emitting diodes (LEDs) centered at 740, 850, and 940 nm (Figure 2B). All derivatives showed strong peak absorption, with extinction coefficients in excess of $1 \times 10^4 \text{ M}^{-1} \cdot \text{cm}^{-1}$ in isobornyl acrylate at the concentration (0.1 mol %) used in the resins for photopolymerization (Table S1 and Figures S4-S14). Brominated azaBODIPYs (R-azaBr) are highlighted in Figure 2B given the precedent for halogenation to improve photopolymerization efficiency.²⁹ However, in-general halogenation of (MeO)_xazaBODIPYs results in a slight blueshift in peak absorption (~10 nm), while no significant change was observed for NMe₂-azaBODIPYs (Figures S15-S19). Increasing the number and strength of EDGs (-OMe to -NMe₂) resulted in a redshift in peak absorbance (λ_{max}), where additional methoxy groups showed a progressive red-shift from bis(H)-azaBr (λ_{max} = 643 nm) to bis(MeO)-azaBr (λ_{max} = 680 nm), and bis(MeO)₃-azaBr (λ_{max} = 694 nm) (Figure S16). Additionally, a >100 nm redshift was observed in going from methoxy- to dimethylamino-functionalized variants (Figure 2B). This dramatic redshift was reported to arise from intramolecular CT between electron-rich amines as donors and the electrondeficient BODIPY core as an acceptor.³¹ In accordance with their absorption spectra, (MeO)_x-azaBODIPYs were primarily assessed as PCs using a far-red LED centered at 740 nm (fwhm

 \approx 36 nm), while NMe₂-azaBODIPYs were examined using NIR LEDs centered at 850 and 940 nm (fwhm \approx 28 and 43 nm, respectively).

Far-Red Photopolymerizations. Each dye was incorporated into a three-component Type II photosystem that we previously developed, 29 where a borate salt served as an electron donor and an iodonium salt an electron acceptor (Figure S1). Photopolymerizations were carried out using 0.1 mol % azaBODIPY, 0.1 mol % donor, and 1.0 mol % acceptor. Isobornyl acrylate was selected as the monomer due to its low volatility and preparation from a renewable resource, borneol (Figure 3A). Two other monomers, 2-hydroxyethyl acrylate and isodecyl acrylate, were also evaluated to examine the versatility of the present photosystem in both hydrophilic and hydrophobic environments, as this has been shown to influence intramolecular CT.³⁷ While both nonpolar and polar monomers could be photopolymerized using the longwavelength irradiation conditions presented herein (Figure S20-S21), for clarity, only the results for isobornyl acrylate are discussed in the main text.

A custom attenuated total reflectance Fourier transform infrared (ATR-FTIR) spectroscopy setup was utilized to monitor the disappearance of C=C double bonds (808 cm⁻¹) resulting from the monomer to polymer conversion (Figure 3A). This setup enables simultaneous LED and IR irradiation from the same face of the crystal, which facilitates precise quantification of photon absorption by minimizing extraneous attenuation from absorption and scattering that would be difficult to avoid from top-down LED illumination. Correspondingly, LED intensity can be tuned to normalize the rate of photon absorption by each photosystem being compared, which allows for the rate of polymerization (r_p) to be directly correlated to the overall reaction efficiency.

Using this setup, the resin was prepared, degassed with argon to remove oxygen, and placed onto the ATR crystal under a blanket of inert gas (Figure S2). This process mitigated oxygen inhibition, providing consistent and reproducible polymerization kinetics. Initially, the effect of azaBODIPY methoxy functionalization on r_p was examined for brominated derivatives and directly compared with (MeO)₃tBu-azaBr as a benchmark that we previously reported.²⁹ Samples irradiated with a far-red LED (λ_{max} = 740 nm) set to a constant intensity of 22 mW/cm² resulted in $r_{\rm p}$ values of 0.187 \pm 0.030, 0.060 \pm 0.007, 0.190 \pm 0.030, and 0.523 ± 0.030 M/s for (MeO)₃tBu-azaBr, bis(H)-azaBr, bis(MeO)-azaBr, and bis(MeO)₃-azaBr, respectively (Figures 3B and S22-S24 and Table S2). The time to reach 50% conversion (t_{50}) was also determined given its relevance to photocuring applications, where ideally this threshold is met in <60 s. The t_{50} values were found to be 11, 42, 10, and 4 s for (MeO)₃tBu-azaBr, bis(H)-azaBr, bis(MeO)-azaBr, and bis-(MeO)₃-azaBr, respectively (Figure 3B and Table S2). Therefore, from an energetic perspective (i.e., constant LED intensity), the addition of methoxy substituents resulted in a clear improvement in efficiency, with a $\sim 3 \times$ increase in rate for bis(MeO)₃-azBr relative to our previously reported derivative, (MeO)₃tBu-azBr.

To gain insights into the intrinsic efficiency of each photosystem (i.e., quantum yield of polymerization), the number of photons absorbed by each resin was matched using LED intensities of 15, 88, 11, and 4 mW/cm² for (MeO) $_3t$ Bu-azaBr, bis(H)-azaBr, bis(MeO)-azaBr, and bis(MeO) $_3$ -azaBr, respectively (Figure S28). This resulted in comparable r_p

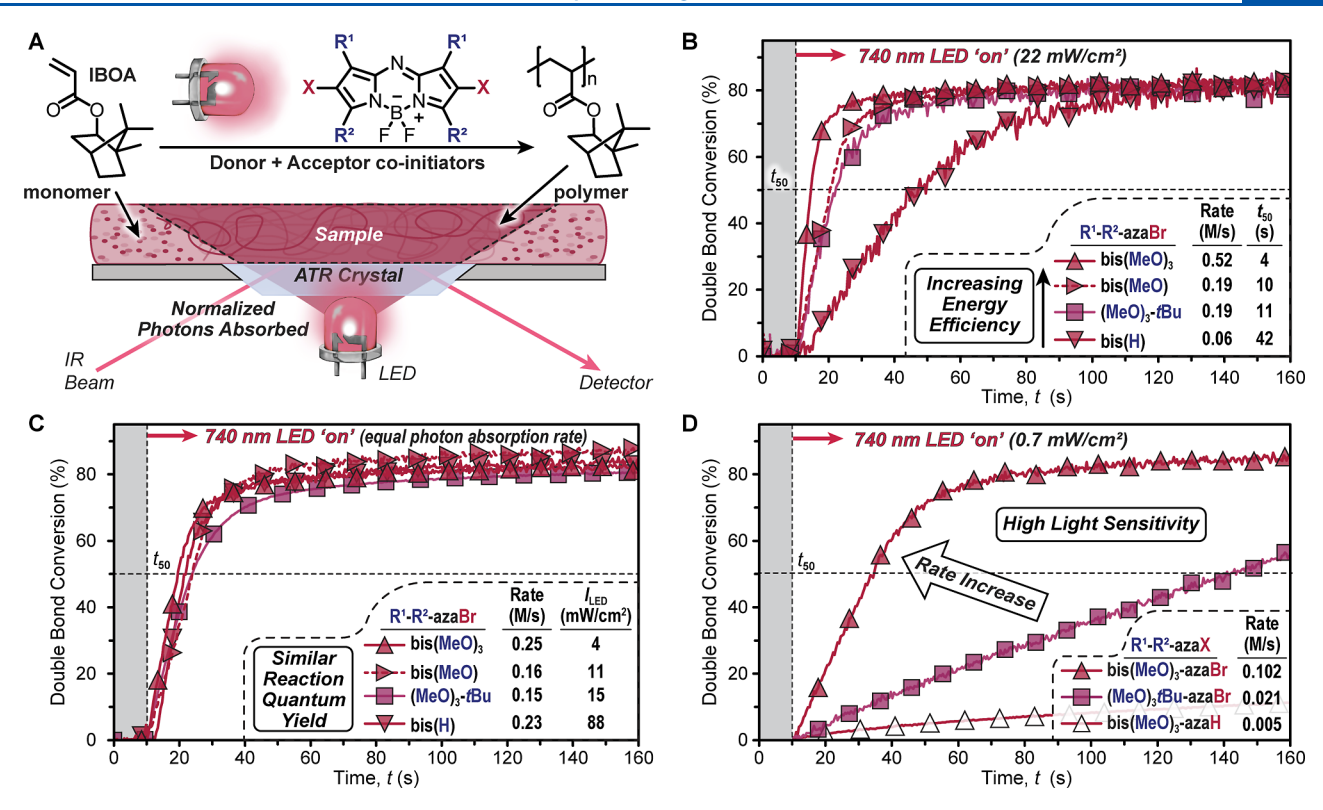


Figure 3. Representative real-time ATR-FTIR analysis of photopolymerizations using azaBOIPY photocatalysts and far-red to NIR LED exposure. (A) Chemical structure for isobornyl acrylate and generic structure for azaBODIPY (0.1 mol %). Borate V served as the electron donor (0.1 mol %) and H-Nu 254 as the electron acceptor (1 mol %). (B) Photopolymerization of (MeO)₃-tBu-azaBr, bis(H)-azaBr, bis(MeO)-azaBr, and bis(MeO)₃-azaBr using a 740 nm LED at an intensity of 22 mW/cm². (C) Photopolymerization of (MeO)₃-tBu-azaBr, bis(H)-azaBr, bis(MeO)-azaBr, and bis(MeO)₃-azaBr using a 740 nm LED whose intensity was set such that each photocatalyst exhibited an identical photon absorption rate. (D) Photopolymerization of (MeO)₃-tBu-azaBr, bis(MeO)₃-azaH, and bis(MeO)₃-azaBr using a 740 nm LED at 0.7 mW/cm².

values of 0.153 ± 0.010 , 0.230 ± 0.020 , 0.156 ± 0.010 , and 0.252 ± 0.006 M/s, respectively (Figure 3C and Table S2). Similar results were also observed for the bis(MeO)_x-azaH series (x = 1, 2, or 3), showing that the trend exists in the absence of halogenation (Figure S29). Therefore, the rate enhancements observed for photopolymerizations with a constant LED intensity were attributed primarily to an increase in absorption and not an increase in polymerization quantum yield, which suggests that each of the brominated derivatives follows the same mechanistic pathway to drive polymerization.

To confirm the effect of halogenation on r_p for the best performing derivative, bis(MeO)3-azaX, resins were assessed and compared with those containing (MeO)₃tBu-azaBr under conditions employing a constant, low LED intensity of 0.7 mW/cm² (Figure 3D) and wherein the light absorption rate of each PC was equalized (Figure S30). This low-intensity performance test is particularly relevant to emergent LCDbased 3D printing processes where intensities on the order of 1 mW/cm² are common.³⁸ Overall, under constant intensity, $k_{\rm p}$ values of 0.021 \pm 0.003, 0.005 \pm < 0.001, and 0.102 \pm 0.006 M/s were measured for (MeO)₃tBu-azaBr, bis(MeO)₃-azaH, and bis(MeO)₃-azaBr, respectively (Figure 3D). Thus, relative to our previously reported derivative, (MeO)₃tBu-azBr, the bis(MeO)₃ analogue provided a ~5× increase in polymerization rate upon exposure to a low-intensity far-red LED, demonstrating higher energy efficiency. Additionally, t_{50} values were 160 and 35 s for (MeO)₃tBu-azaBr and bis(MeO)₃-azaBr, respectively, under these same conditions (Figure 3D, dashed line). Furthermore, tuning the light intensity to provide equal photon absorption rates for all resins revealed a ~4× faster

polymerization for bis $(MeO)_3$ -azaBr relative to bis $(MeO)_3$ -azaH (Figure S30), which was attributed to the heavy-atom effect that we previously reported.²⁹

NIR Photopolymerizations. Next, we sought to leverage stronger EDGs, specifically tertiary amines, to further redshift the absorption of azaBODIPYs and produce PCs that react under NIR light (>780 nm). Figure 4A shows absorption spectra of bis(NMe₂)-azaH, tBu-NMe₂-azaH, and NMe₂-tBu-azaH, which each display two bands, a high-energy one (λ_{max} < 650 nm) assigned to a π - π * transition and a low-energy one that arises from an intramolecular CT transition. Notably, positioning the -NMe₂ substituents on the top phenyl rings results in a stronger bimodal absorption band and a slight blue shift in the CT band.

Using an 850 nm LED at an intensity of 55 mW/cm², k_p values of 0.099 \pm 0.002, 0.11 \pm 0.01, and 0.013 \pm 0.001 M/s and t_{50} values of 27, 25, and 144 s were measured, respectively, for bis(NMe₂)-azaH, tBu-NMe₂-azaH, and NMe₂-tBu-azaH (Figure 4B and Table S2). We also demonstrated that bis(NMe₂)-azaH and its brominated analogue, bis(NMe₂)azaBr, polymerized upon exposure to a 940 nm LED, although halogenation of these BODIPY derivatives did not improve the polymerization efficiency (Figure S32 and Table S2). The apparent lack of a heavy-atom effect may arise from low triplet energies that do not effectively facilitate electron transfer. Notably, the exposure of resins containing bis(MeO)₃-azaBr to the 940 nm LED did not result in photopolymerization. In contrast, with bis(NMe2)-azaH, full conversion was achieved in 50 s upon irradiation with an 850 nm LED at 55 mW/cm² and in 90 s under irradiation with a 940 nm LED at the same

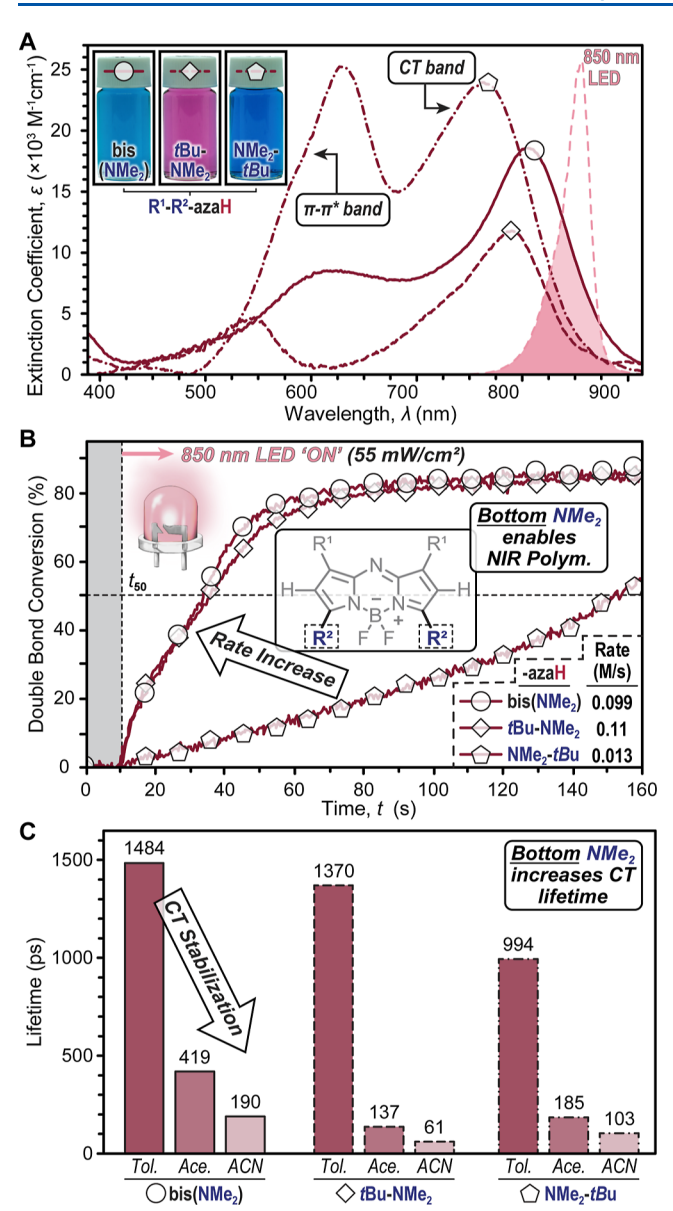


Figure 4. Characterization of NIR-absorbing bis(NMe₂)-azaH, tBu-NMe₂-azaH, and NMe₂-tBu-azaH BODIPYs. (A) Absorbance profiles in isobornyl acrylate (0.1 mol %) and 850 nm LED profile, with shaded regions showing overlap between them. (B) Photopolymerization rates using an 850 nm LED at 55 mW/cm². (C) Extracted S₁ state lifetimes from TA spectroscopy as a function of solvent polarity. Tol. = toluene; Ace. = acetone; and ACN = acetonitrile.

power density. Overall, these results validate our central hypothesis. The addition of strong EDGs to the azaBODIPY scaffold can indeed be used to produce effective NIR PCs, with polymerization rates hitting the $\sim\!0.1$ M/s benchmark. However, the photopolymerization rates for the NMe₂-azaBODIPYs did not appear to correlate solely with NIR LED absorption, which necessitated additional spectroscopic characterization.

To gain insights into the dynamic excited state mechanism(s) governing NIR photopolymerization efficiency, we conducted TA measurements on bis(NMe₂)-azaH, tBu-NMe₂-azaH, and NMe₂-tBu-azaH. Samples of each compound were prepared in three solvents of different polarities, toluene (dielectric constant, $\kappa = 2.38$), acetone ($\kappa = 20.7$), and acetonitrile ($\kappa = 37.5$), which were chosen due to their

differing expected abilities to stabilize CT states (details on TA measurements, spectral interpretations, and modeling procedures can be found in the Supporting Information).

Upon photoexcitation, each of the NMe₂-azaBODIPY derivatives was found to produce a TA signal that decayed over time with negligible spectral evolution (Figures S45–S47). This indicated that the electronic state (S_1) produced by photoexcitation decays directly to the ground state without producing other states (e.g., triplets). Extracting S_1 state lifetimes from the TA signals revealed a strong dependence on the solvent polarity for all three derivatives. For example, $tBu-NMe_2$ -azaH's S_1 state persists for 1.37 ns in nonpolar toluene, but its lifetime is shortened substantially to 137 and 61 ps in polar acetone and acetonitrile, respectively. We attribute the correlation between decreasing solvent polarity and enhanced azaH S_1 lifetime to the CT character of the S_1 state. Polar solvents stabilize the CT state, which, according to the energy gap law, promotes a faster relaxation to the ground state.

Notably, bis(NMe₂)- and tBu-NMe₂-azaH exhibited S₁ lifetimes in toluene that were ~1.5× longer than the S₁ lifetime of NMe₂-tBu-azaH. This result correlates with the photopolymerization kinetics observed in nonpolar IBOA resins, where those containing bis(NMe₂)- and tBu-NMe₂-azaH are nearly 10× faster than with NMe₂-tBu-azaH. However, the longer excited state lifetime may only partially account for the notable improvement in r_p , and we thus speculate that there may be other factors at play, such as a smaller energetic driving force for electron transfer when placing NMe₂ functionality on the "top" half of the BODIPY structure and/or steric encumberance mitigating redox when bulky tBu functionality is present on the "bottom" half of the BODIPY structure.

CONCLUSIONS

The incorporation of electron-donating groups on azaBODIPY dyes was demonstrated to be an effective strategy to improve the energy efficiency of far-red-to-NIR light-induced polymerizations without the need for large extensions of π -conjugation. Overall, far-red photopolymerizations with (MeO)_x-azaBODI-PY derivatives generally benefited from an increase in the number of electron-donating methoxy substituents (x), due to a redshift in absorption and halogenation, which was attributed to an increased excited state lifetime. Together, these strategies provided good photocatalyst solubility and enabled photopolymerizations at a monomer conversion rate of 0.1 M/s upon exposure to a far-red 740 nm LED with very low light intensity (0.7 mW/cm²). Furthermore, (NMe)₂-azaBODIPYs that contained stronger EDGs benefited from enhanced CT character that increased their NIR absorption and enabled fast polymerizations (\sim 0.1 M/s) upon exposure to an 850 nm LED at modest intensity (55 mW/cm²). Ground state and TA spectroscopy revealed that the placement of (NMe)2 functionality on the BODIPY core ("top" vs "bottom" half of the structure) significantly influenced the CT character, revealing a direct correlation between CT excited state lifetime and photopolymerization rate. This result suggested that longer excited state lifetimes facilitated photoredox to induce polymerization. However, further photophysical studies are warranted to determine the significance of this kinetic effect relative to other energetic and steric factors that may additionally influence the photopolymerization rate. Overall, the findings from this study show that azaBODIPYs are effective far-red and NIR photoredox catalysts that enable

rapid polymerization, while intramolecular CT can additionally facilitate this objective. Going forward, the present structure—reactivity relationships will guide the design of more efficient photoredox catalysts, along with those that absorb further red and/or dissolve in water to enable the preparation of hydrogels. These design principles will also inform the development of NIR photoredox catalysts for advanced manufacturing. Specifically, given the demonstrated rates (\sim 0.1 M/s) at low light intensities (\lesssim 50 mW/cm²), the present photosystem can enable low-energy photocuring technologies, such as projection-based 3D printing, to fabricate, for example, high-resolution composites for aerospace and cell-laden hydrogels for regenerative medicine.

ASSOCIATED CONTENT

5 Supporting Information

The Supporting Information is available free of charge at https://pubs.acs.org/doi/10.1021/acs.macromol.3c02004.

Materials and methods, equipment and instrumentation, absorption spectroscopy, and material characterization (PDF)

AUTHOR INFORMATION

Corresponding Authors

Sean T. Roberts — Department of Chemistry, The University of Texas at Austin, Austin, Texas 78712, United States; orcid.org/0000-0002-3322-3687; Email: roberts@cm.utexas.edu

Zachariah A. Page — Department of Chemistry, The University of Texas at Austin, Austin, Texas 78712, United States; orcid.org/0000-0002-1013-5422; Email: zpage@utexas.edu

Authors

Alex Stafford — Department of Chemistry, The University of Texas at Austin, Austin, Texas 78712, United States Seth R. Allen — Department of Chemistry, The University of Texas at Austin, Austin, Texas 78712, United States; orcid.org/0000-0003-1511-6594

Laura Estergreen — Department of Chemistry, The University of Texas at Austin, Austin, Texas 78712, United States;
orcid.org/0000-0003-2534-534X

Kristina Kafle – Department of Chemistry, The University of Texas at Austin, Austin, Texas 78712, United States

Complete contact information is available at: https://pubs.acs.org/10.1021/acs.macromol.3c02004

Author Contributions

Conceptualization (AS and ZAP); methodology (AS, SRA, LE, STR, and ZAP); investigation (AS, SRA, KK, and LE); visualization (AS, SRA, STR, and ZAP); funding acquisition (STR, and ZAP); project administration (STR, and ZAP); supervision (STR, and ZAP); writing—original draft (AS, STR, and ZAP); and writing—review and editing (AS, SRA, STR, and ZAP).

Notes

The authors declare no competing financial interest.

ACKNOWLEDGMENTS

The authors acknowledge primary support from the Department of Defense under Grant no. W911NF2210115 (A.S., K.K., and Z.A.P.; synthesis, steady-state characterization,

photopolymerizations, and materials and supplies). Partial support was provided by the National Science Foundation under Grant no. CAT-2155017 (S.R.A., L.E., S.T.R., and Z.A.P.; TA spectroscopy), the Welch Foundation under Grant no. F-2007 (Z.A.P.) and F-1885 (S.T.R.), and Research Corporation for Science Advancement under Award #28184 (Z.A.P.). We acknowledge Kristina Kafle for the TOC graphic.

ABBREVIATIONS

NIR, near-infrared; PET, photoinduced electron/energy transfer; UV, ultraviolet; BODIPY, boron dipyromethene; LED, light-emitting diode; $r_{\rm p}$, polymerization rate; I, light intensity; $\lambda_{\rm max}$, wavelength maximum; ISC, intersystem crossing; EDG, electron-donating group; PC, photocatalyst; CT, charge transfer; fwhm, full width at half-maximum; ATR, attenuated total reflectance; FTIR, Fourier transform infrared; TA, transient absorption

REFERENCES

- (1) Kocaarslan, A.; Tabanli, S.; Eryurek, G.; Yagci, Y. Near-Infrared Free-Radical and Free-Radical-Promoted Cationic Photopolymerizations by In-Source Lighting Using Upconverting Glass. *Angew. Chem., Int. Ed.* **2017**, *56*, 14507–14510.
- (2) Fagnani, D. E.; Tami, J. L.; Copley, G.; Clemons, M. N.; Getzler, Y. D. Y. L.; McNeil, A. J. 100th Anniversary of Macromolecular Science Viewpoint: Redefining Sustainable Polymers. *ACS Macro Lett.* **2021**, *10*, 41–53.
- (3) Lee, Y.; Boyer, C.; Kwon, M. S. Visible-Light-Driven Polymerization towards the Green Synthesis of Plastics. *Nat. Rev. Mater.* **2021**, *7*, 74–75.
- (4) Dumur, F. Recent Advances on Photoinitiating Systems Designed for Solar Photocrosslinking Polymerization Reactions. *Eur. Polym. J.* **2023**, *189*, 111988.
- (5) Wallin, T. J.; Pikul, J.; Shepherd, R. F. 3D Printing of Soft Robotic Systems. *Nat. Rev. Mater.* 2018, 3, 84–100.
- (6) Ligon, S. C.; Liska, R.; Stampfl, J.; Gurr, M.; Mülhaupt, R. Polymers for 3D Printing and Customized Additive Manufacturing. *Chem. Rev.* **2017**, *117*, 10212–10290.
- (7) Bagheri, A.; Jin, J. Photopolymerization in 3D Printing. ACS Appl. Polym. Mater. 2019, 1, 593-611.
- (8) Truby, R. L.; Lewis, J. A. Printing Soft Matter in Three Dimensions. *Nature* **2016**, *540*, *371*–*378*.
- (9) Murphy, C. A.; Lim, K. S.; Woodfield, T. B. F. Next Evolution in Organ-Scale Biofabrication: Bioresin Design for Rapid High-Resolution Vat Polymerization. *Adv. Mater.* **2022**, *34*, 2107759.
- (10) Zou, X.; Zhu, J.; Zhu, Y.; Yagci, Y.; Liu, R. Photopolymerization of Macroscale Black 3D Objects Using Near-Infrared Photochemistry. *ACS Appl. Mater. Interfaces* **2020**, *12*, 58287–58294.
- (11) Lu, P.; Ahn, D.; Yunis, R.; Delafresnaye, L.; Corrigan, N.; Boyer, C.; Barner-Kowollik, C.; Page, Z. A. Wavelength-Selective Light-Matter Interactions in Polymer Science. *Matter* **2021**, *4*, 2172–2229
- (12) Atchison, J.; Kamila, S.; Nesbitt, H.; Logan, K. A.; Nicholas, D. M.; Fowley, C.; Davis, J.; Callan, B.; McHale, A. P.; Callan, J. F. Iodinated Cyanine Dyes: A New Class of Sensitisers for Use in NIR Activated Photodynamic Therapy (PDT). *Chem. Commun.* **2017**, *53*, 2009–2012.
- (13) Borjigin, T.; Schmitt, M.; Giacoletto, N.; Rico, A.; Bidotti, H.; Nechab, M.; Zhang, Y.; Graff, B.; Morlet-Savary, F.; Xiao, P.; Dumur, F.; Lalevée, J. The Blue-LED-Sensitive Naphthoquinone-Imidazolyl Derivatives as Type II Photoinitiators of Free Radical Photopolymerization. *Adv. Mater. Interfaces* **2023**, *10*, 2202352.
- (14) Pang, Y.; Jiao, H.; Zou, Y.; Strehmel, B. The NIR-Sensitized Cationic Photopolymerization of Oxetanes in Combination with Epoxide and Acrylate Monomers. *Polym. Chem.* **2021**, *12*, 5752–5759.

- (15) Wang, Q.; Popov, S.; Strehmel, V.; Gutmann, J. S.; Strehmel, B. NIR-Sensitized Hybrid Radical and Cationic Photopolymerization of Several Cyanines in Combination with Diaryliodonium Bis-(Trifluoromethyl)Sulfonyl Imide. *Polym. Chem.* **2023**, *14*, 116–125.
- (16) Topa-Skwarczyńska, M.; Galek, M.; Jankowska, M.; Morlet-Savary, F.; Graff, B.; Lalevée, J.; Popielarz, R.; Ortyl, J. Development of the First Panchromatic BODIPY-Based One-Component Iodonium Salts for Initiating the Photopolymerization Processes. *Polym. Chem.* **2021**, *12*, 6873–6893.
- (17) Ma, Q.; Liu, S.; Le Dot, M.; Mokbel, H.; Zhang, Y.; Graff, B.; Lalevée, J. Imidazole Based Dual Photo/Thermal Initiators for Highly Efficient Radical Polymerization under Air with a Metal-Free Approach. *Polym. Chem.* **2021**, *12*, 6386–6391.
- (18) Dumur, F. The Future of Visible Light Photoinitiators of Polymerization for Photocrosslinking Applications. *Eur. Polym. J.* **2023**, *187*, 111883.
- (19) Fors, B.; Trotta, J. Organic Catalysts for Photocontrolled Polymerizations. *Synlett* **2016**, *27*, 702–713.
- (20) Stafford, A.; Allen, S. R.; Grusenmeyer, T. A.; O'Dea, C. J.; Estergreen, L.; Roberts, S. T.; Page, Z. A. Thiophene-Fused Boron Dipyrromethenes as Energy Efficient near-Infrared Photocatalysts for Radical Polymerizations. J. Mater. Chem. A 2023, 11, 22259–22266.
- (21) Ahn, D.; Stevens, L. M.; Zhou, K.; Page, Z. A. Rapid High-Resolution Visible Light 3D Printing. ACS Cent. Sci. 2020, 6, 1555–1563.
- (22) Ahn, D.; Stevens, L. M.; Zhou, K.; Page, Z. A. Additives for Ambient 3D Printing with Visible Light. *Adv. Mater.* **2021**, 33, 2104906.
- (23) Stevens, L. M.; Tagnon, C.; Page, Z. A. Invisible" Digital Light Processing 3D Printing with Near Infrared Light. ACS Appl. Mater. Interfaces 2022, 14, 22912–22920.
- (24) Corrigan, N.; Yeow, J.; Judzewitsch, P.; Xu, J.; Boyer, C. Seeing the Light: Advancing Materials Chemistry through Photopolymerization. *Angew. Chem., Int. Ed.* **2019**, *58*, 5170–5189.
- (25) Xiao, P.; Zhang, J.; Dumur, F.; Tehfe, M. A.; Morlet-Savary, F.; Graff, B.; Gigmes, D.; Fouassier, J. P.; Lalevée, J. Visible Light Sensitive Photoinitiating Systems: Recent Progress in Cationic and Radical Photopolymerization Reactions under Soft Conditions. *Prog. Polym. Sci.* **2015**, 41, 32–66.
- (26) Bonardi, A. H.; Dumur, F.; Grant, T. M.; Noirbent, G.; Gigmes, D.; Lessard, B. H.; Fouassier, J. P.; Lalevée, J. High Performance Near-Infrared (NIR) Photoinitiating Systems Operating under Low Light Intensity and in the Presence of Oxygen. *Macromolecules* **2018**, *51*, 1314–1324.
- (27) Bonardi, A.; Bonardi, F.; Noirbent, G.; Dumur, F.; Dietlin, C.; Gigmes, D.; Fouassier, J. P.; Lalevée, J. Different NIR Dye Scaffolds for Polymerization Reactions under NIR Light. *Polym. Chem.* **2019**, 10, 6505–6514.
- (28) Zhou, J.; Pitzer, L.; Ley, C.; Rölle, T.; Allonas, X. A Highly Sensitive Photoinitiating System Based on Pre-Associated Ion-Pairs for NIR Radical Photopolymerization of Optically Clear Materials. *Polym. Chem.* **2022**, *13*, 6475–6483.
- (29) Stafford, A.; Ahn, D.; Raulerson, E. K.; Chung, K. Y.; Sun, K.; Cadena, D. M.; Forrister, E. M.; Yost, S. R.; Roberts, S. T.; Page, Z. A. Catalyst Halogenation Enables Rapid and Efficient Polymerizations with Visible to Far-Red Light. *J. Am. Chem. Soc.* **2020**, *142*, 14733–14742.
- (30) Xu, Y.; Zhao, M.; Zou, L.; Wu, L.; Xie, M.; Yang, T.; Liu, S.; Huang, W.; Zhao, Q. Highly Stable and Multifunctional Aza-BODIPY-Based Phototherapeutic Agent for Anticancer Treatment. ACS Appl. Mater. Interfaces 2018, 10, 44324–44335.
- (31) Obłoza, M.; Łapok, Ł.; Pędziński, T.; Stadnicka, K. M.; Nowakowska, M. Synthesis, Photophysics and Redox Properties of Aza-BODIPY Dyes with Electron-Donating Groups. *ChemPhysChem* **2019**, 20, 2482–2497.
- (32) Zhao, J.; Xu, K.; Yang, W.; Wang, Z.; Zhong, F. The Triplet Excited State of Bodipy: Formation, Modulation and Application. *Chem. Soc. Rev.* **2015**, *44*, 8904–8939.

- (33) Lu, P.; Chung, K. Y.; Stafford, A.; Kiker, M.; Kafle, K.; Page, Z. A. Boron Dipyrromethene (BODIPY) in Polymer Chemistry. *Polym. Chem.* **2021**, *12*, 327–348.
- (34) Lakshmi, V.; Rajeswara Rao, M.; Ravikanth, M. Halogenated Boron-Dipyrromethenes: Synthesis, Properties and Applications. *Org. Biomol. Chem.* **2015**, *13*, 2501–2517.
- (35) Shi, Z.; Han, X.; Hu, W.; Bai, H.; Peng, B.; Ji, L.; Fan, Q.; Li, L.; Huang, W. Bioapplications of small molecule Aza-BODIPY: from rational structural design to *in vivo* investigations. *Chem. Soc. Rev.* **2020**, 49, 7533–7567.
- (36) Rana, P.; Singh, N.; Majumdar, P.; Prakash Singh, S. Evolution of BODIPY/Aza-BODIPY Dyes for Organic Photoredox/Energy Transfer Catalysis. *Coord. Chem. Rev.* **2022**, *470*, 214698.
- (37) Uddin, A.; Allen, S. R.; Rylski, A. K.; O'Dea, C. J.; Ly, J. T.; Grusenmeyer, T. A.; Roberts, S. T.; Page, Z. A. Do The Twist: Efficient Heavy-Atom-Free Visible Light Polymerization Facilitated by Spin-Orbit Charge Transfer Inter-System Crossing. *Angew. Chem., Int. Ed.* 2023, 62, No. e202219140.
- (38) Stevens, L. M.; Recker, E. A.; Zhou, K. A.; Garcia, V. G.; Mason, K. S.; Tagnon, C.; Abdelaziz, N.; Page, Z. A. Counting All Photons: Efficient Optimization of Visible Light 3D Printing. *Adv. Mater. Technol.* **2023**, 2300052.